

# Fault-Tolerant Variable Speed Limit Control for Freeway Work Zone

Shuming Du, Saiedeh Razavi  
McMaster University, Hamilton, Ontario, Canada  
dus5@mcmaster.ca

**Abstract.** Freeway work zone can easily lead to traffic congestion which has detrimental effects on travel time and safety. By using the detected traffic states near work zone area, variable speed limit (VSL) control system has been widely studied to improve traffic mobility and safety. However, occurrence of sensor fault can cause traffic state deviation and system degradation. Therefore, this study presents a fault-tolerant VSL control system for freeway work zone. A traffic flow model was first designed to analyze the traffic dynamics. Then a sliding mode controller for VSL was designed based on the previous study. By comparing the estimated traffic states from Kalman filter with the observed states from the observer, the developed fault diagnosis can detect the sensor fault and reconfigure the controller. The proposed system was evaluated under a realistic freeway work zone environment in traffic simulator SUMO. The results show the proposed system can achieve fault tolerance and improve traffic mobility and safety under fault-free and sensor-fault scenarios.

## 1. Introduction

With the aging of road infrastructure, a large number of work zones are setup up for highway maintenance projects such as road reconstruction, resurfacing and rehabilitation. Despite the long term benefit from road maintenance projects, work zones with lane closure in these projects exacerbate traffic congestion and increase the safety risk near work zone area. In 2014, around 888 million hours delay, 90 thousand crashes and 600 fatalities occurring in US are attributed to work zones (FHWA, 2014). To reduce the impacts of freeway work zone, variable speed limit (VSL) control system has been studied. By dynamically changing the speed limits upstream of a work zone bottleneck, VSL control system can restrict the traffic inflow or improve the traffic homogenization so as to improve traffic mobility and safety.

To design the VSL control system, a number of approaches have been developed. By using the detected traffic density near work zone area, the proportional-integral (PI) feedback VSL controller was designed by Carlson et al. (2011) to regulate the mainline traffic flow. This method was also applied to multiple bottlenecks (Iordanidou et al., 2017). The model predictive control method was developed to improve the performance of VSL control system using macroscopic model and microscopic model respectively (Hegyi et al., 2005; Du et al., 2017). Although the improved system performance with reduced travel time and safety risk is shown by using VSL systems in the abovementioned studies, the potential sensor fault is not considered. The implementation of such VSL systems is mainly based on an assumption that accurate traffic state measurement is available. However, in reality, the stationary sensors such as loop detectors, video cameras and magnetic sensors suffer from different types of sensor faults. Approximately 40% of the traffic data is missing due to the sensor malfunction in California (Rajagopal et al., 2007). Therefore, without consideration of the sensor fault, the performance of VSL control system can be highly unpredictable and it may cause safety issues with an improper VSL control scheme.

In the case of sensor faults, the redundancy of the control system is exploited to achieve the fault tolerance and maintain the system performance. Two types of redundancies, physical redundancy and analytical redundancy, are commonly utilized in control systems (Blanke et

al., 2006). Since the physical redundancy demands additional components to be installed, it is hardly affordable to use such fault tolerance due to its extra cost in a large scale system like freeway in this study. However, the analytical redundancy is analyzed and extracted from the mathematical system model, whereby the dependability of a system is improved with little additional cost. Therefore, the analytical redundancy is mainly discussed and studied.

Various studies have developed traffic data imputation methods to overcome the issue of traffic sensor faults. A tensor decomposition based method was developed to recover the missing traffic data (Tan et al., 2013). By training the model using a deep learning algorithm, Duan et al. (2016) presented a well-trained model for traffic data imputation. However, these traffic imputation approaches are implemented offline and cannot recover the missing data in real time. Since VSL control systems require real-time traffic state estimation or imputation when sensor fault occurs, it is difficult to incorporate offline imputation methods in the design of VSL control system. Many online imputation methods were also proposed. The corrupted traffic data is estimated using the linear regression model (Chen et al., 2003). Iterative multiple imputation method was developed to predict the missing traffic data pattern via a calibrated regression model (Henrickson et al., 2015). Zhang and Zhang (2016) proposed two multivariate forecasting methods based on regression models to forecast the missing traffic data. Nevertheless, large historical data samples are required to calibrate the abovementioned regression models before being used to recover the missing data online. However, when there is a work zone, particularly a short-term work zone, set up in the freeway, such historical traffic data is normally not available. Consequently, it is also difficult to apply aforementioned online imputation methods to VSL control system for freeway work zone.

To overcome the impacts of sensor faults, this study presents a fault-tolerant VSL control system for freeway work zone. Two main contributions are made: 1) maintain the VSL control performance with the occurrence of sensor faults; 2) achieve sensor fault diagnosis online using the observer-based method without the requirement of large historical data samples. Therefore, the developed system has the following objectives: 1) accurately estimate the traffic states using stationary sensors and probe sensors; 2) develop a VSL controller based on the previous study; 3) design a fault diagnosis scheme to achieve fault detection and model reconfiguration; 4) evaluate the designed system using a realistically simulated freeway work zone environment in traffic simulator SUMO.

The rest of this paper is organized as follows. The system framework is first described. Based on the designed traffic flow model, a sliding mode controller is introduced for VSL control. Then Kalman filter is employed to estimate the traffic states. After the design of the observer, fault diagnosis scheme is discussed. Afterwards, the developed system is evaluated with analytical results. Finally, conclusions and future work are discussed.

## **2. Methodology**

The framework of the designed fault-tolerant VSL control system is shown in Figure 1. The sliding mode controller is designed to generate the speed limit signal in order to track the traffic state reference and improve traffic condition near work zone area. Then this speed limit signal is incorporated in the traffic flow model to affect the evolution of the traffic states. With traffic measurements from stationary sensors and probe sensors, Kalman filter is employed to improve the accuracy of the traffic states estimation. Traffic measurements are also sent to the designed observer to generate the observed traffic states as the redundant information. Then both estimated traffic states from Kalman filter and observed traffic states from the observer are fed into the fault diagnosis to detect whether a sensor fault occurs and

reconfigure the controller accordingly. The details of each component in Figure 1 are presented in the following sections.

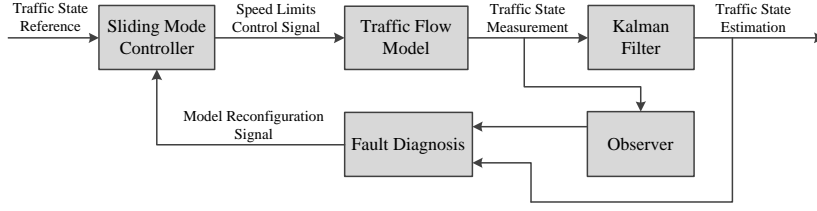


Figure 1: System Framework

## 2.1 Traffic Flow Model

The layout of freeway work zone with lane closure is shown in Figure 2. The mix traffic flow with conventional and connected vehicles moves towards the right side. Connected vehicles used in this study have the ability to transmit their positions and speeds during the travel while conventional vehicles do not have the communication ability. The driver behavior between conventional vehicles and connected vehicles is assumed to be the same. Traffic states are detected using stationary sensors and probe sensors. Stationary sensors are installed at fixed locations to detect traffic states and connected vehicles are utilized as probe sensors. In the case of stationary sensors, two traffic sensors TS 1 and TS 2, which are located immediate upstream of the work zone and within work zone area respectively, are used. It can be seen that congestion can easily occur when traffic demand exceeds the work zone capacity.

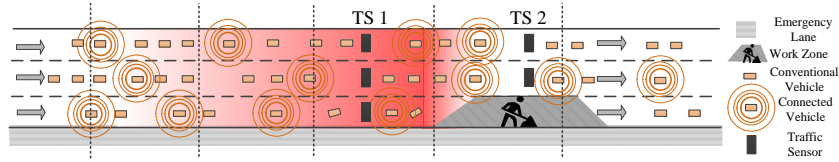


Figure 2: Layout of Freeway Work Zone Area

To analyze the traffic dynamics near work zone area, the layout of freeway work zone area is partitioned into multiple segments as shown in Figure 3.

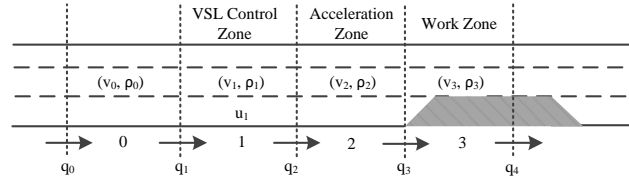


Figure 3: Segments of Freeway Work Zone Area

The traffic flow rate  $q_i$  and  $q_{i+1}$  are the inflow and outflow for segment  $i$ . The length of each segment, average speed and density in segment  $i$  are expressed as  $L_i$ ,  $v_i$  and  $\rho_i$  respectively. Traffic sensor TS 1 and TS 2 are located inside acceleration zone and work zone respectively. One speed limit sign is installed at the beginning of the VSL control zone to control vehicle speed within VSL control zone. Another speed limit sign is installed at the start of the acceleration zone to allow vehicles to accelerate and travel through the work zone area with maximum free flow speed. In this study, we assume no congestion happens downstream of the work zone.

Based on the conservation law (Daganzo 1994), the evolution of traffic density is derived as

$$\rho_i(k+1) = \rho_i(k) + \frac{\Delta T_s}{L_i} [q_i(k) - q_{i+1}(k)], i = 0, 1, 2, 3 \quad (1)$$

where  $\Delta T_s$  is the sample time interval and  $k$  stands for the discrete time step  $k$ . Since the objective of VSL controller is to control the traffic density of the acceleration zone (Du and Razavi, 2019), traffic flow  $q_2, q_3$  and  $q_4$  are obtained in Equation (2) under the assumption of triangular fundamental diagram

$$\begin{cases} q_2(k) = \min\{v_1(k)\rho_1(k), \frac{\omega\rho_j u_1(k)}{u_1(k) + \omega}, \omega(\rho_j - \rho_2(k))\} \\ q_3(k) = \min\{v_2(k)\rho_2(k), \beta C^b\} \\ q_4(k) = v_3(k)\rho_3(k) \end{cases} \quad (2)$$

where  $\omega$  and  $\rho_j$  represent the backward wave speed and jam density respectively.  $u_1(k)$  is the speed limit of VSL control zone.  $C^b$  is the work zone bottleneck capacity which equals to 2/3 of full road capacity  $C$  as one of three lanes is closed shown in Figure 3. The capacity drop phenomenon occurs when a queue forms upstream of the work zone (Hall et al., 1992; Chung et al., 2007). This can further decrease the work zone bottleneck capacity  $C^b$ . Therefore, a capacity drop factor  $\beta$  is introduced when capacity drop occurs.

As we can see, the impact of speed limits on traffic flow is reflected by the term  $q_2^u(k) = \omega\rho_j u_1(k) / [u_1(k) + \omega]$ . When  $v_1(k)\rho_1(k) < q_2^u(k)$ , traffic demand is lower than the work zone capacity  $C^b$  and vehicles can travel through the work zone area with free flow speed. Therefore, VSL controller is not needed to restrict the traffic flow with speed limits. On the other hand, when  $\omega(\rho_j - \rho_2(k)) < q_2^u(k)$ , the VSL controller cannot restrict the traffic flow. This conflicts with the stability of VSL controller discussed in the sliding mode controller section. Therefore, the evolution of traffic density  $\mathbf{x}(k)$  is derived as

$$\mathbf{x}(k+1) = \mathbf{A}(k)\mathbf{x}(k) + \mathbf{B}(k)\mathbf{u}(k) + \boldsymbol{\varepsilon}(k) \quad (3)$$

where  $\mathbf{u}(k)$  is the system input and  $\boldsymbol{\varepsilon}(k)$  is the system process noise which is assumed to be Gaussian noise of zero mean and covariance  $\mathbf{Q}(k)$ .  $\mathbf{A}(k)$  and  $\mathbf{B}(k)$  are system matrices. More specifically, Equation (3) can be rewritten as

$$\begin{bmatrix} \rho_2(k+1) \\ \rho_3(k+1) \end{bmatrix} = \begin{bmatrix} 1 - \frac{\Delta T_s}{L_2} v_2(k) & 0 \\ \frac{\Delta T_s}{L_3} v_2(k) & 1 - \frac{\Delta T_s}{L_3} v_3(k) \end{bmatrix} \begin{bmatrix} \rho_2(k) \\ \rho_3(k) \end{bmatrix} + \begin{bmatrix} \frac{\Delta T_s}{L_2} q_2^u(k) \\ 0 \end{bmatrix} + \begin{bmatrix} \varepsilon_1(k) \\ \varepsilon_2(k) \end{bmatrix} \quad (4)$$

$$\begin{bmatrix} \rho_2(k+1) \\ \rho_3(k+1) \end{bmatrix} = \begin{bmatrix} 1 & 0 \\ 0 & 1 - \frac{\Delta T_s}{L_3} v_3(k) \end{bmatrix} \begin{bmatrix} \rho_2(k) \\ \rho_3(k) \end{bmatrix} + \begin{bmatrix} \frac{\Delta T_s}{L_2} (q_2^u(k) - \beta C^b) \\ \frac{\Delta T_s}{L_3} \beta C^b \end{bmatrix} + \begin{bmatrix} \varepsilon_1(k) \\ \varepsilon_2(k) \end{bmatrix} \quad (5)$$

Equation (4) and (5) are derived under without capacity drop and with capacity drop scenarios respectively. The average speed  $v_2(k)$  and  $v_3(k)$  are detected by connected vehicles.

Meanwhile, the stationary sensors TS 1 and TS 2 can be used to detect the traffic flow. Thus the measurement equation is derived as

$$\mathbf{y}(k) = \mathbf{C}(k)\mathbf{x}(k) + \boldsymbol{\zeta}(k) \quad (6)$$

where  $\mathbf{y}(k)$  is the measurement vector and  $\boldsymbol{\zeta}(k)$  is the measurement noise assumed to be Gaussian noise of zero mean and covariance  $\mathbf{R}(k)$ . Specifically, Equation (6) is written as

$$\begin{bmatrix} q_3(k) \\ v_2(k) \\ q_4(k) \\ v_3(k) \end{bmatrix} = \begin{bmatrix} 1 & 0 \\ 0 & 1 \end{bmatrix} \begin{bmatrix} \rho_2(k) \\ \rho_3(k) \end{bmatrix} + \begin{bmatrix} \zeta_1(k) \\ \zeta_2(k) \end{bmatrix} \quad (7)$$

where traffic flow  $q_3(k)$  and  $q_4(k)$  are detected by the stationary sensor TS 1 and TS 2.

By combining Equation (3) and (6), the traffic flow model is established.

## 2.2 Sliding Mode Controller

The sliding mode controller, which is a non-linear control strategy for VSL control, can generate switching control signal to drive the traffic state to the desired equilibrium state with certain convergence rates. The objective of the designed controller is to stabilize the traffic density  $\rho_2$  at the bottleneck critical density  $\rho_c^b = C^b / v_f$  where  $v_f$  is the free flow speed. Through this stabilization, the capacity drop is avoided and the maximum flow rate can be achieved. The designed controller is based on the previous study (Du and Razavi, 2019).

The desired equilibrium state  $\rho_c^b$  is first designed on the sliding surface as:

$$s(k) = c[\rho_c^b - \rho_2(k)] \quad (8)$$

where  $c$  is a constant nonzero parameter. The reaching process, which is designed as Equation (9) is utilized to drive the traffic state towards the surface (Gao et al., 1995).

$$s(k+1) = s(k) - \Delta T_s \eta \operatorname{sgn}(s(k)) - \Delta T_s q s(k) \quad (9)$$

where both  $\eta$  and  $q$  are positive constant parameters. The term  $\Delta T_s q s(k)$  can make the traffic state move towards the surface at exponential convergence rate, while the term  $\Delta T_s \eta \operatorname{sgn}(s(k))$  can make the traffic state converge to equilibrium state with finite time steps.

Therefore, the traffic density  $\rho_2(k+1)$  can be derived from the perspective of the controller design by combining the Equation (8) at time step  $k+1$  with Equation (9). On the other hand, the traffic density  $\rho_2(k+1)$  can also be obtained from the perspective of the traffic dynamics in Equation (3) which contains the control signal  $u_1(k)$ . Thus combining these two densities  $\rho_2(k+1)$  gives a function  $g$  of speed limit control signal  $u_1(k)$  as

$$u_1(k) = g(\rho_2(k), v_2(k), s(k)) \quad (10)$$

The stability of the designed controller is guaranteed with the condition that  $\eta > 0$ ,  $q > 0$  and  $2 - \Delta T_s q \gg 0$  which is proved in the previous study (Du and Razavi, 2019). Also, different convergence rates should be designed for with and without capacity drop scenarios. The reason is that the major consideration for VSL controller under different scenarios is different (Du and Razavi, 2019). A quick response is needed when there is no capacity drop, while an overshoot issue should be avoided when capacity drop occurs.

To apply the speed limit control in real world, three speed constraints are considered: 1) only discrete speed limits between maximum legitimate speed limit  $v_{\max}$  and minimum speed limit

$v_{\min}$  with the increment speed  $\Delta v$  are displayed; 2) the continuous speed limit is rounded up to its closed discrete speed limit; 3) the maximum speed difference is limited to  $\Delta v_{\max}$  between two consecutive control time step.

### 2.3 Kalman Filter for Traffic State Estimation

Kalman filter is a dynamic estimation algorithm with time update and measurement update (Bar-Shalom et al., 2001). The following update equations are used to estimate traffic states

$$\mathbf{x}(k+1|k) = \mathbf{A}(k)\mathbf{x}(k) + \mathbf{B}(k)\mathbf{u}(k) \quad (11)$$

$$\mathbf{P}(k+1|k) = \mathbf{A}(k)\mathbf{P}(k)\mathbf{A}(k)^T + \mathbf{Q}(k) \quad (12)$$

$$\mathbf{K}(k) = \mathbf{P}(k+1|k)\mathbf{C}(k)^T(\mathbf{C}(k)\mathbf{P}(k+1|k)\mathbf{C}(k)^T + \mathbf{R}(k))^{-1} \quad (13)$$

$$\mathbf{x}(k+1) = \mathbf{x}(k+1|k) + \mathbf{K}(k)(\mathbf{y}(k) - \mathbf{C}(k)\mathbf{x}(k+1|k)) \quad (14)$$

$$\mathbf{P}(k+1) = (\mathbf{I} - \mathbf{K}(k)\mathbf{C}(k))\mathbf{P}(k+1|k) \quad (15)$$

With the one step prediction of state  $\mathbf{x}(k+1|k)$  and state covariance  $\mathbf{P}(k+1|k)$ , the filter gain  $\mathbf{K}(k)$  is updated. By incorporating the error between the measurements and one step prediction, the state  $\mathbf{x}(k+1)$  along with the state covariance  $\mathbf{P}(k+1)$  at next time step are updated. Then this recursive process is performed to update and estimate the traffic density with new measurements at each time step.

### 2.4 Observer

The observer can provide the redundant traffic state to achieve fault tolerance. It can be seen that traffic density  $\rho_2(k)$  is critical to the design of sliding mode controller. Consequently, a faulty traffic sensor TS 1, which can provide the measurement of  $\rho_2(k)$  via the detection of traffic flow, can greatly affect the VSL control. Therefore, the observer should provide the observed traffic density  $\rho_2^o(k)$  when traffic sensor TS 1 fails.

**Observability.** When TS 1 fails, Equation (6) is modified as  $\rho_3(k) = \mathbf{C}^o(k)\mathbf{x}(k) + \zeta_2(k)$  where  $\mathbf{C}^o(k) = [0 \ 1]$  and  $\zeta_2(k)$  is the Gaussian noise with zero mean and variance  $R_2(k)$ . Then the observability matrix  $\mathbf{O}_{\text{no,drop}}$  and  $\mathbf{O}_{\text{drop}}$  for without capacity drop and with capacity drop scenarios respectively are derived as

$$\mathbf{O}_{\text{no,drop}} = \begin{bmatrix} 0 & 1 \\ \frac{\Delta T_s}{L_3} v_{n+2}(k) & 1 - \frac{\Delta T_s}{L_3} v_3(k) \end{bmatrix}, \mathbf{O}_{\text{drop}} = \begin{bmatrix} 0 & 1 \\ 0 & 1 - \frac{\Delta T_s}{L_3} v_3(k) \end{bmatrix} \quad (16)$$

When  $v_2(k) \neq 0$ ,  $\mathbf{O}_{\text{no,drop}}$  has full rank. Accordingly, traffic density  $\rho_2(k)$  is observable when capacity drop does not occur, while  $\rho_2(k)$  is non-observable with capacity drop.

**Observer Design.** In the case of the scenario without capacity drop, since  $\rho_2(k)$  is observable, the observed density  $\rho_2^o(k)$  can be obtained using the Kalman recursive algorithm which acts as an observer instead of a filter. By replacing  $\mathbf{C}(k)$ ,  $\mathbf{y}(k)$  and  $\mathbf{R}(k)$  in Equation (13)-(15) with  $\mathbf{C}^o(k)$ ,  $\rho_3(k)$  and  $R_2(k)$  respectively, the Kalman recursive process is performed using

Equation (11)-(15) to obtain the observed  $\rho_2^o(k)$ . When capacity drop occurs, the recursive process cannot be used as  $\rho_2(k)$  is non-observable. However, the error of one-step prediction does not diverge with capacity drop. Therefore, an open loop estimator with one-step prediction using Equation (11) is utilized to obtain the observed traffic density  $\rho_2^o(k)$ .

## 2.5 Fault Diagnosis

The observer-based method is employed to design the fault diagnosis. By utilizing the observer discussed in Section 2.4, the designed fault diagnosis can detect the sensor fault, and then reconfigure the VSL controller when a fault occurs. This study focuses on the stationary sensor fault, specifically traffic sensor TS 1 which is critical to the design of VSL controller. There are different types of sensor faults. For example, the fault with the detection of zero flow rate is the leading fault among the malfunctions in loop detectors (Chen et al., 2003). Therefore, the malfunction TS 1 of zero flow rate is mainly considered in this study.

The residual between the estimated density  $\hat{\rho}_2(k)$  and the observed density  $\rho_2^o(k)$  is analyzed to achieve fault detection. The residual  $r_d$  for traffic density  $\rho_2(k)$  is derived as

$$r_d = \frac{|\hat{\rho}_2(k) - \rho_2^o(k)|}{\lambda \rho_c^b} \quad (17)$$

where  $\lambda$  is a constant parameter. When there is no sensor fault, the estimated  $\hat{\rho}_2(k)$  will be closed to the observed  $\rho_2^o(k)$ . Then a small residual can be obtained. However, a sensor fault can cause a large residual due to the abnormal deviation of  $\hat{\rho}_2(k)$ . Therefore, a threshold  $\tau$  is determined as a comparison to achieve fault detection.  $\lambda$  and  $\tau$  are selected considering model uncertainties and noises.

After the detection of a sensor fault, the fault diagnosis can reconfigure the controller. Without sensor fault, the estimated density can be used in the design of VSL controller. However, when a sensor fault occurs, the estimated density will greatly deviate from the actual density. To maintain the control system performance, the fault diagnosis can reconfigure the controller by replacing the estimated density with the observed density.

## 3. Experiment and Results

The developed fault-tolerant VSL control for freeway work zone was evaluated on a 4.8 km (3 mi) freeway segment of I-15S in California, US. A work zone was set up from State PM (postmile) 40.2 to State PM 37.6 on July 22, 2016. This freeway segment with the work zone is shown in Figure 4. The blue line represents the simulated freeway segment, while the red line shows part of the work zone where one of three lanes was closed. The freeway network was built in traffic simulator SUMO. The microscopic model was calibrated and validated using realistic traffic measurements from California freeway database (PeMS, 2016).



Figure 4: Freeway Network with Work Zone

With the built traffic network, the fundament diagram was calibrated. The road capacity  $C$ , jam density  $\rho_j$ , the critical density  $\rho_c^b$ , free flow speed  $v_f$ , backward propagating wave speed  $\omega$ , capacity drop factor  $\beta$  are calibrated as 4800 veh/h, 270 veh/km, 35 veh/km, 108 km/h, 21 km/h and 0.94 respectively. Without the loss of generality, the length of each segment is selected same as 500 m. The method proposed in this study can potentially be extended to different lengths of segments. According to the realistic traffic data statistics analysis (Bekiaris-Liberis, et al., 2016), the standard deviation of the noises of stationary sensors and probe sensors were selected as 25 veh/h and 3 km/h respectively. The connected market penetration rate was chosen as 20%. The speed limits  $v_{\max}$ ,  $v_{\min}$ ,  $\Delta v$  and  $\Delta v_{\max}$  were 113 km/h (70 mi/h), 16 km/h (10 mi/h), 8 km/h (5 mi/h) and 16 km/h (10 mi/h) respectively. For the controller, two sets of parameters  $c_1 = 2, \eta = 6, q_1 = 15$  and  $c_1 = 10, \eta = 50, q_1 = 90$  were selected for without capacity drop and with capacity drop scenarios respectively. The 15 s sample time interval and 30 s control time interval were selected.  $\lambda = 2$  and  $\tau = 0.5$  were chosen. Different combinations of  $\lambda$  and  $\tau$  were tested in this study to find the appropriate value, whereby a fault can be accurately detected without a false alarm.

The developed fault-tolerant control system was evaluated under three scenarios: 1) without control; 2) with fault-tolerant control but no sensor fault occurs; 3) with fault-tolerant control but TS 1 fails during the simulation. The simulation was first run for 5 minutes as the warm-up period with low traffic demand. This 5-minute traffic data was discarded. Then 1 h simulation was conducted. During this 1 h simulation, an average low demand 1500 veh/h was first generated until the time 400 s, then there was an average high demand 3600 veh/h lasting for 1100 s, followed by low demand 1500 veh/h for the rest 2100 s. An artificial sensor fault occurred at the time step 1200 s under scenario 3.

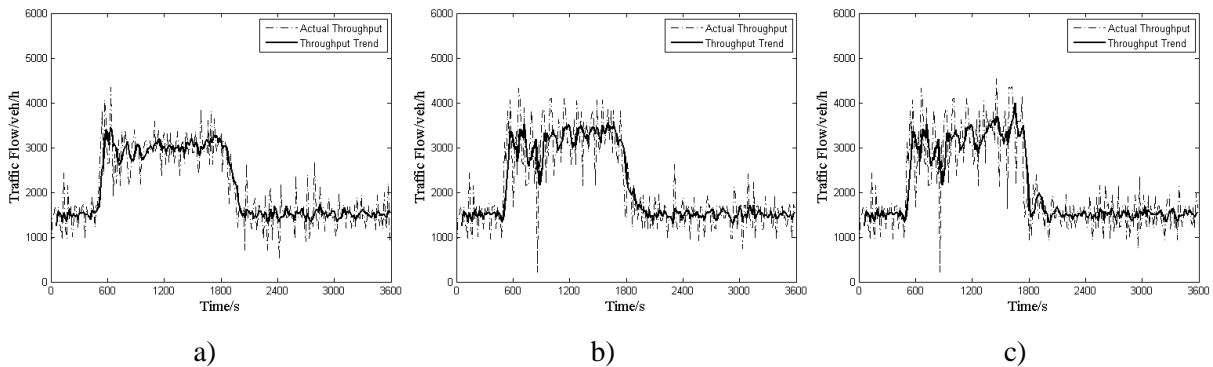


Figure 5: Work Zone Throughput under a) Scenario 1; b) Scenario 2; c) Scenario 3

The work zone throughputs under three scenarios are illustrated in Figure 5. The actual throughput in dash line is collected by TS 2 every sample time interval, while the throughput trend in solid line is presented using moving average technique. Without VSL control, the capacity drop occurs in Figure 5a with a throughput of about 3000 veh/h during the high demand. In contrast, throughputs under scenario 2 and 3 stay around 3200 veh/h which is the work zone capacity under high demand. Though the throughput slightly drops for a short time near time step 900 s due to the initiation of VSL, the overall throughput successfully maintains at the work zone capacity. The similar performance between Figure 5b and 5c after 1200 s when the sensor fault occurs shows the effectiveness of fault-tolerant control.

The residual and traffic density at acceleration zone under scenario 2 and 3 are presented in Figure 6 and 7 respectively. It can be seen that the developed system shows the ability to achieve density estimation and fault tolerance. Under scenario 2, the residual stays below the threshold all the time without false alarm. The density estimation is compared with the ground

truth measurement from the simulator in Figure 6b. An accurate density estimation is achieved with the RMSE of 3.9 veh/km. In Figure 7a, the residual exceeds the threshold at the time step 1200 s when the sensor fails. Then the density estimation greatly deviates from the measurement in Figure 7b. However, the observed traffic density in blue line comes into effect and replaces the corrupted density estimation. Thus the fault tolerance can be achieved.

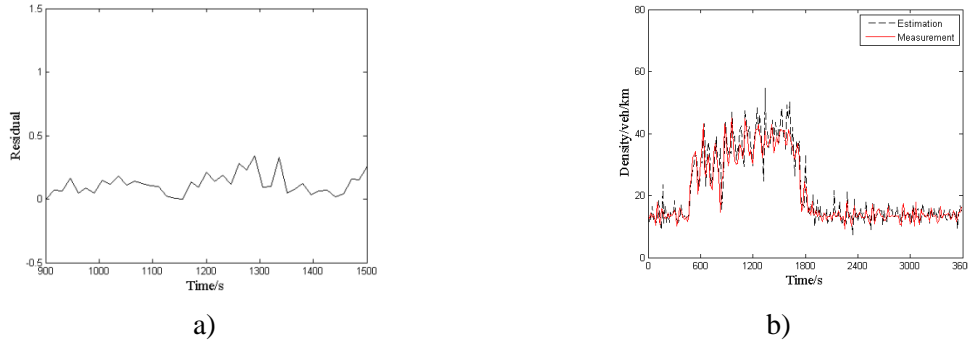


Figure 6: Under Scenario 2 a) Residual; b) Density at Acceleration Zone

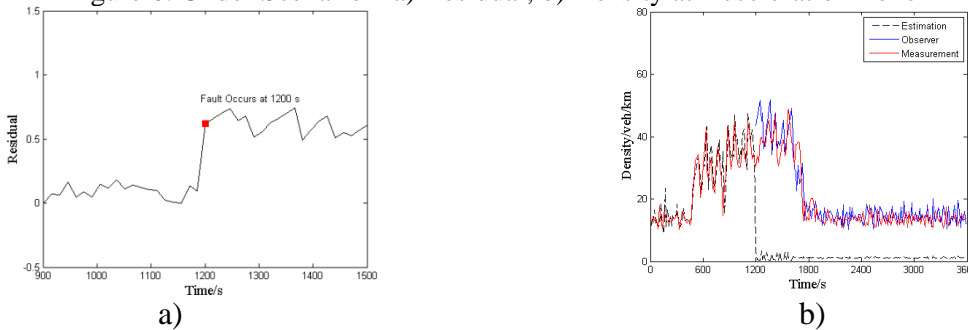


Figure 7: Under Scenario 3 a) Residual; b) Density at Acceleration Zone

Table 1: Performance Measurement

Scenario	Travel Time $T$ /min	Improvement/%	Time-to-collision $p$ /%	Improvement/%
1	2.30	-	4.43	-
2	2.11	8.26	0.42	90.5
3	2.10	8.70	0.41	90.7

The travel time  $T$  and probability of time-to-collision  $p$  are presented in Table 1. Only the travel time upstream of the work zone is considered. 1.5 s is used as the minimum time to avoid the collision (Genders and Razavi, 2016). Table 1 shows the developed system can not only improve the mobility and safety by around 8% and 90% respectively near work zone area, but also achieve fault tolerance with the similar system performance under scenario 3.

The results indicate that the developed fault-tolerant VSL control system can avoid the capacity drop phenomenon occurring near freeway work zone area and improve the mobility and safety at the same time. More importantly, the system can achieve fault tolerant control and maintain the system performance with the presence of a sensor fault.

#### 4. Conclusions and Future Work

To ensure the effectiveness of VSL control and avoid system degradation when a sensor fault occurs, a fault-tolerant VSL control system for freeway work zone is developed in this study. Accurate traffic density estimation is achieved by employing Kalman filter. Meanwhile, the sliding mode controller for VSL control can avoid the capacity drop and improve traffic mobility and safety for freeway work zone. Furthermore, the developed fault diagnosis can not only detect a sensor fault but also reconfigure the controller accordingly. The designed

fault-tolerant VSL control shows the ability to consistently improve the traffic condition near freeway work zone area even with a sensor fault.

In this study, only the stationary sensor fault is considered. However, the faults of connected vehicles such as the communication delay and corrupted samples can also affect the VSL control performance. Probe sensor faults will be considered in the future. Meanwhile, the impacts of different connected vehicle market penetration rates will also be studied. Mobile applications as another type of probe sensors will be considered for fault detection as well.

## References

- Bar-Shalom, Y., Li, X. R. and Kirubarajan, T. (2001). *Estimation with Applications to Tracking and Navigation: Theory, Algorithms, and Software*. New York: Wiley.
- Bekiaris-Liberis, N., Roncoli, C. and Papageorgiou, M. (2016). Highway Traffic State Estimation with Mixed Connected and Conventional Vehicles. *IEEE Trans. Intell. Transp. Syst.*, 17(12), 3484–3497.
- Blanke, M., Kinnaert, M., Lunze, J. and Staroswiecki, M. (2006). *Diagnosis and Fault-Tolerant Control*. 2nd ed. Berlin: Springer.
- Carlson, R. C., Papamichail, I. and Papageorgiou, M. (2011). Local Feedback-based Mainstream Traffic Flow Control on Motorways Using Variable Speed Limits. *IEEE Trans. Intell. Transp. Syst.*, 12(4), 1261–1276.
- Chen, C., Kwon, J., Rice, J., Skabardonis, A. and Varaiya, P. (2003). Detecting Errors and Imputing Missing Data for Single-Loop Surveillance Systems. *Transp. Res. Rec.*, (1855), 160–167.
- Chung, K., Rudjanakanoknad, J. and Cassidy, M.J. (2007). Relation Between Traffic Density and Capacity Drop at Three Freeway Bottlenecks. *Transp. Res. Part B Methodol.*, 41, 82–95.
- Daganzo, C. F. (1994). The Cell Transmission Model: A Dynamic Representation of Highway Traffic Consistent with the Hydrodynamic Theory. *Transp. Res. Part B Methodol.*, 28(4), 269–287.
- Du, S., Razavi, S. and Genders, W. (2017). Optimal Variable Speed Limit Control under Connected Work Zone and Connected Vehicle Environment. In *Proc., 34th Int. Symp. Automat. Robotics in Construction, June 2017*, Taipei, Taiwan: IAARC.
- Du, S. and Razavi, S. (2019). Variable Speed Limit for Freeway Work Zone with Capacity Drop Using Discrete-Time Sliding Mode Control. *J. Comput. Civ. Eng.*, 33(2):04019001.
- Duan, Y., Lv, Y., Liu, Y.L. and Wang, F. (2016). An Efficient Realization of Deep Learning for Traffic Data Imputation. *Transp. Res. Part C Emergin Technol.*, 72, 168–181.
- FHWA (2014). Work Zone Management Program. [Viewed 1 March 2019]. Available from: [https://ops.fhwa.dot.gov/wz/resources/facts\\_stats.htm](https://ops.fhwa.dot.gov/wz/resources/facts_stats.htm).
- Gao, W., Wang, Y. and Homaifa, A. (1995). Discrete-time Variable Structure Control Systems. *IEEE Trans. Ind. Electron.*, 42(2), 117–122.
- Genders, W. and Razavi, S. (2016). Impact of Connected Vehicle on Work Zone Network Safety through Dynamic Route Guidance. *J. Comput. Civ. Eng.*, 30(2):04015020.
- Hall, F. L., Hurdle, V. F. and Banks, J. H. (1992). Synthesis of Recent Work on the Nature of Speed-flow and Flow-occupancy (or density) Relationships on Freeways. *Transp. Res. Rec.*, 1365, 12–18.
- Hegy, A., De Schutter, B. and Hellendoorn, J. (2005). Optimal Coordination of Variable Speed Limits to Suppress Shock Waves. *IEEE Trans. Intell. Transp. Syst.*, 6(1), 102–112.
- Henrickson, K., Zou, Y. and Wang, Y. (2015). Flexible and Robust Method for Missing Loop Detector Data Imputation. *Transp. Res. Rec.*, (2527), 29–36.
- Iordanidou, G. R., Papamichail, I., Roncoli, C. and Papageorgiou, M. (2017). Feedback-based Integrated Motorway Traffic Flow Control with Delay Balancing. *IEEE Trans. Intell. Transp. Syst.*, 18 (9), 2319–2329.
- PeMS. (2016). Caltrans Performance Measurement System. [Viewed 1 March 2019]. Available from: <http://pems.dot.ca.gov>.
- Rajagopal, R. and Varaiya, P. (2007). Evaluating the Health of California Loop Sensor Network. Transportation Research Board, Washington DC.
- Tan, H., Feng, G., Feng, J., Wang, W., Zhang, Y.J. and Li, F. (2013). A Tensor-based Method for Missing Traffic Data Completion. *Transp. Res. Part C Emergin Technol.*, 28, 15–27.
- Zhang Y. and Zhang Y. (2016). A Comparative Study of Three Multivariate Short Term Freeway Traffic Flow Forecasting Methods With Missing Data. *J. Intell. Transp. Syst.*, 20(3), 205-218.